Measurement for Complex Magnetic Fields

Masashi Kawakami*, Fengchao Xiao*, Kimitoshi Murano†, and Yoshio Kami*

*University of Electro-Communications, Japan, Email: {kawakami, xiao, kami}@ice.uec.ac.jp
†Tokai University, Japan, Email: {murano@dj.u-tokai.ac.jp

***Abstract*—In the field of EMC, if electromagnetic fields could be measured with both the magnitude and the phase, i.e. in complex value, the generation and propagation mechanisms of emissions in electric equipment would become clear in detail, thus more effective information would be offered for designing circuit boards and chassis. In this paper, a technique to measure the complex magnetic field near a circuit board using a 6-port circuit is discussed. To examine the proposed technique, some simulation results are shown.**

***Index Terms*—Complex magnetic field, magnetic near-field measurement, EMI, 6-port circuit.**

I. Introduction

Electromagnetic interference (EMI) problem is due to complex issues, and is one of the difficult tasks for electromagnetic compatibility (EMC) research. The radiation source in electronic equipments may be the longest traces on a printed circuit board (PCB), or the current flowing through the wiring of the active component, such as the ICs. One way for considering the radiaton mechanism from this sourse is measuring the near magnetic field [1]-[7]. In [7], photoelectronic elements were used for measuring magnetic fileds. Magnetic field probes based on Faraday's law of induction have also been developed based on the semiconductor technology, and put into practical uses. In [4] and [5], an approach of estimating the electric field from the measured magnetic fields as in the finite-difference time-domain (FDTD) method was proposed. In [8] a method of visualizing the Poynting and wavenumber vectors was discussed. For estimating the power flow, the electromagnetic fields should be measured in complex values. In [9] where the complex electromagnetic fields near circuits board was measured using a 6-port circuit. The 6-port has two input ports and four output ports and the complex input voltage (current) at the input ports are estimated from the power measured at the output ports. This work is based on the research in [9], but a wide-range measurement method is proposed by applying the idea of a circuit concept, the final purpose of this rsearch is to estimate the power flow that reveals the direction of electromagnetic wave propagation. To examine the proposed technique, some simulation results are shown.

II. Principle 6-port based on the circuit concept

The 6-port circuit proposed by Engen [10] is a multiport circuit, two input ports and four output ports. It is known that 6-port circuit can be used as network analyzers and correlators [10]-[11]. The four output signals are the combinations of the two input signals with different weighting magnitude/phase coefficients. This allows the input complex signals to be estimated from the analog signals (powers) measured at the output ports. 6-port circuit is generally constructed by hybrids and dividers. The characteristics of the hybrid circuit elements determine the frequency characteristics and operation band of the 6-port. In this research, a 2-input and 4-output circuit like the conventional 6-port circuit is used, but by applying the idea of a circuit concept, a wide-range measurement method is proposed.

Assuming a black box with two input ports connected to the voltage sources (signal generator) and four output ports terminated with loads ($R_0 = 50\ \Omega$ in our study) for power measurement, as shown in Fig. 1. This network aim to measure the amplitudes and phases of the voltage sources connected to the input ports. There is four unknowns in the voltage sources, and this four unknowns will be estimated from the four measured analog values (powers). In the actural cases, one of the input ports is assumed to be reference port, and this network estimates the amplitude ratio and phase difference.

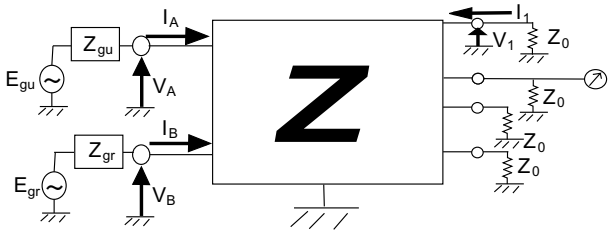

Fig. 1. The equivalent circuit of a 6-port.

If the impedance matrix $\boldsymbol{Z}$ of the black box is known,

$$\boldsymbol{V} = \boldsymbol{Z}\boldsymbol{I} \tag{1}$$

where $\boldsymbol{V} = [V_u, V_r, V_1, \cdots, V_4]^T$, $\boldsymbol{I} = [I_u, I_r, I_1, \cdots, I_4]^T$ are vectors of terminal voltages and currents. The input port as reference is denoted with subscript r, and the under test port is denoted with subscript u, and the output ports are denoted with subscript $i = 1, 2, 3, 4$. The terminal condition cab be given as

$$\boldsymbol{V} = \boldsymbol{E} - \boldsymbol{R}\boldsymbol{I} \tag{2}$$

where $\boldsymbol{R}$ is a 6×6 terminal load impedance matrix with the main diagonal elements corresponding to the load impedances of each ports or internal impedances of the sources, and other elements of zero, $\boldsymbol{E}$ is the terminal voltage vector which elements are the source voltages connecting to each ports. From (1) and (2), the terminal currents vector $\boldsymbol{I}$ are

$$\boldsymbol{I} = (\boldsymbol{R} + \boldsymbol{Z})^{-1}\boldsymbol{E} \equiv \boldsymbol{Y}\boldsymbol{E} \tag{3}$$

where $\mathbf{Y}$ is a 6×6 admittance matrix. From (3), the currents at the output ports can be expressed as

$$I_i = Y_{ir}E_r + Y_{iu}E_u, \qquad i = 1, 2, 3, 4 \tag{4}$$

Let $Y_{iu} = |Y_{iu}|e^{j\phi_{iu}}$, $Y_{ir} = |A_{ir}|e^{j\phi_{ir}}$, and the sources $E_u = |E_u|e^{j\theta_u}$, $E_r = |E_r|e^{j\theta_r}$, then (4) can be further expressed as

$$I_i = |Y_{iu}||E_u|e^{j(\phi_{iu}+\theta_u)} + |Y_{ir}||E_r|e^{j(\phi_{ir}+\theta_r)} \tag{5}$$

For the power at the output ports terminated with loads ($R_0 = 50\ \Omega$), we have

$$\begin{aligned} P_i &= R_0 I_i I_i^* = R_0 |I_i|^2 \\ &= R_0 ||Y_{iu}||E_u| \{\cos(\phi_{iu} + \theta_u) + j\sin(\phi_{iu} + \theta_u)\} \\ &\quad + |Y_{ir}||E_r|\{\cos(\phi_{ir} + \theta_r) + j\sin(\phi_{ir} + \theta_r)\}|^2 \\ &= R_0 \left[|Y_{iu}|^2|E_u|^2 + |Y_{ir}|^2|E_r|^2 \right. \\ &\quad + 2|Y_{iu}||Y_{ir}||E_u||E_r| \{\cos(\theta_u - \theta_r)\cos(\phi_{iu} - \phi_{ir}) \\ &\quad \left. - \sin(\theta_u - \theta_r)\sin(\phi_{iu} - \phi_{ir})\}\right] \\ &\equiv a_i|E_u|^2 + b_i|E_r|^2 + c_i|E_u||E_r|\cos\theta \\ &\quad + d_i|E_u||E_r|\sin\theta \end{aligned} \tag{6}$$

where $\theta = \theta_u - \theta_r$ is the phase difference between the two input sources. Let $\phi_i \equiv \phi_{iu} - \phi_{ir}$, then the coefficients in (6) are

$$\begin{aligned} a_i &= R_0|Y_{iu}|^2 \\ b_i &= R_0|Y_{ir}|^2 \\ c_i &= 2R_0|Y_{iu}||Y_{ir}|\cos\phi_i \\ d_i &= -2R_0|Y_{iu}||Y_{ir}|\sin\phi_i \end{aligned} \tag{7}$$

As long as the impedance matrix of the black box is known, all these coefficients can be easily calculated from the above equations. By permutation with (6) we have,

$$\begin{bmatrix} |E_u|^2 \\ |E_r|^2 \\ |E_u||E_r|\cos\theta \\ |E_u||E_r|\sin\theta \end{bmatrix} = \begin{bmatrix} a_1 & b_1 & c_1 & d_1 \\ a_2 & b_2 & c_2 & d_2 \\ a_3 & b_3 & c_3 & d_3 \\ a_4 & b_4 & c_4 & d_4 \end{bmatrix}^{-1} \begin{bmatrix} P_1 \\ P_2 \\ P_3 \\ P_4 \end{bmatrix} \tag{8}$$

Thus if the power at the output ports are measured, then the amplitude ratio and phase difference between the two signal sources can be estimated. Let

$$\begin{bmatrix} Q_1 \\ Q_2 \\ Q_3 \\ Q_4 \end{bmatrix} = \begin{bmatrix} a_1 & b_1 & c_1 & d_1 \\ a_2 & b_2 & c_2 & d_2 \\ a_3 & b_3 & c_3 & d_3 \\ a_4 & b_4 & c_4 & d_4 \end{bmatrix}^{-1} \begin{bmatrix} P_1^m \\ P_2^m \\ P_3^m \\ P_4^m \end{bmatrix} \tag{9}$$

where P_i^m $(i = 1, 2, 3, 4)$ are the measured power at the four output ports respectively, then the amplitude ratio and phase difference between the two signal sources are estimated as

$$\frac{|E_u|}{|E_r|} = \sqrt{\frac{Q_1}{Q_2}} \tag{10}$$

$$arg(\frac{E_u}{E_r}) = \tan^{-1}\left(\frac{Q_4}{Q_3}\right) \tag{11}$$

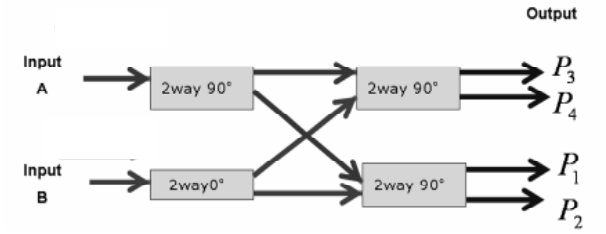

Fig. 2. The block diagram of 6-port A.

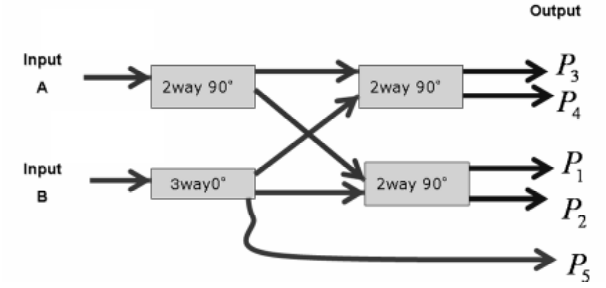

Fig. 3. The block diagram of 6-port B.

III. Testing 6-port circuits

For confirm the above discussions, two 6-port circuits, denoted as 6-port A and B, have been fabricated, and the block diagrams are shown in Figs. 2 and 3. 6-port A as shown in Fig. 2 is based on the 6-port circuit used in [9], and the 6-port B as shown in Fig. 3 is similar to the 6-port circuit proposed by Engen [10]. The circuit in Fig. 3 is actually having 7 ports, thus port 1 is always terminated with a load in our study and the power at this port is not necessary. Both the two 6-ports are faricated with the surface mount power splitters with the operating frequency band of 800 to 900 MHz according to the specifications.

For obtaining the impedance matrix of the 6-port, the S parameters of the 6-ports are measured using a network analyzer. The impedance matrix can be derived from the S parameters as

$$\boldsymbol{Z} = R_0(\boldsymbol{E} - \boldsymbol{S})^{-1}(\boldsymbol{E} + \boldsymbol{S}) \tag{12}$$

where $\boldsymbol{E}$ is a 6×6 unit matrix. Assuming the two inputs of the 6-ports are of same amplitude of 10 mV, and in phase, the power at the four ports are calculated from (6) and (12) with the measured S parameters. Then the amplitude ratio and phase difference between the two signal sources are estimated. The results are shown in Figs. 4 and 5. Both the two 6-ports estimated the amplitude ratio and phase difference well.

However, noise in the actual power measurements is unavoidable due to the accuracy of the measuring instruments and the measurement errors. Thus simulations were conducted with the power at port 2 having a 0.1 dBm measurement errors, and the estimated results are shown in Figs. 6 and 7. One can see 6-port A is very sensitive to the errors, both the amplitude ratio and phase difference are not correctly estimated. On the

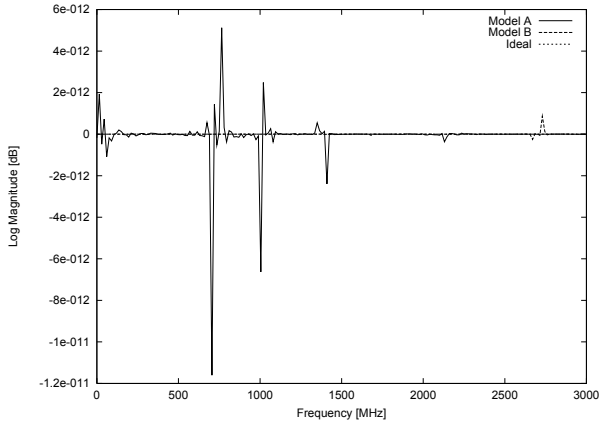

Fig. 4. Simulation results for the amplitude ratio by using the measured S paramteres of the 6-ports.

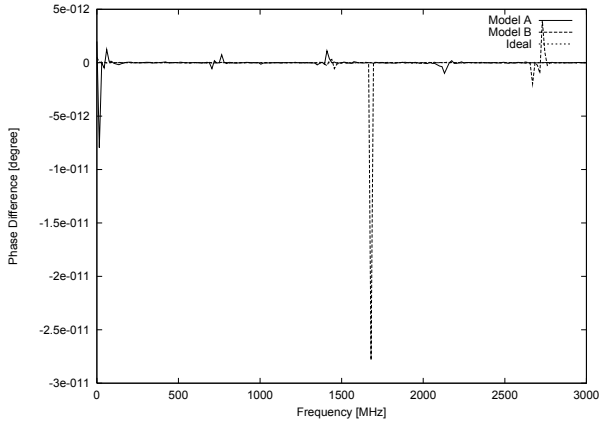

Fig. 5. Simulation results for the phase difference by using the measured S paramteres of the 6-ports.

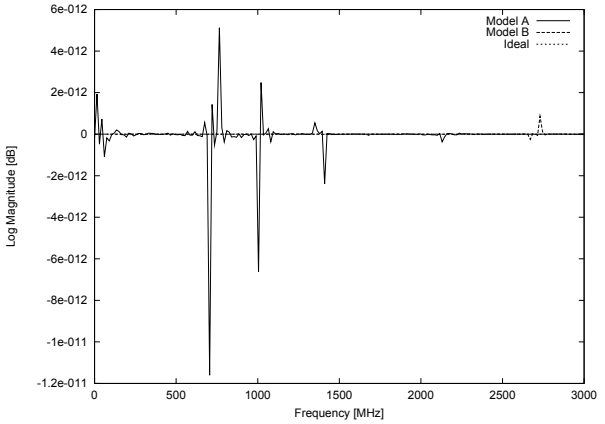

Fig. 6. Simulation results for the amplitude ratio with 0.1 dBm measurement errors at port 2.

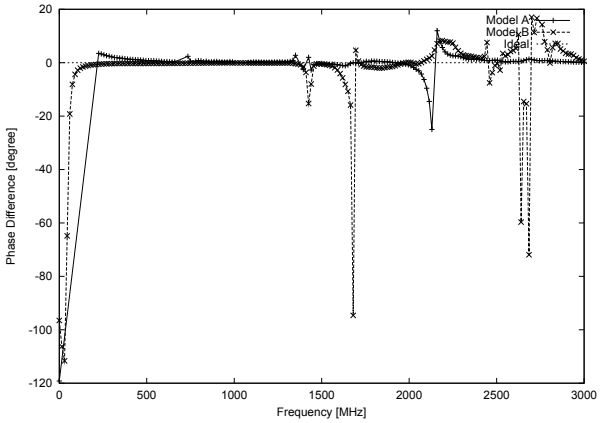

Fig. 7. Simulation results for the phase difference with 0.1 dBm measurement errors at port 2.

other hand, 6-port B can estimate the amplitude ratio and phase difference fairly well.

For investigating why two 6-ports have different performances, the S parameters of the 6-ports are calculated by assuming the power splitters being ideal devices. Then the coefficient matrices which is used in (8) for inversion have been calculated. For 6-port A, this matrix is

$$\mathbf{K}_{sa} = R_0 \cdot 10^{-4} \begin{bmatrix} \frac{1}{4} & \frac{1}{4} & \frac{1}{2} & 0 \\ \frac{1}{4} & \frac{1}{4} & -\frac{1}{2} & 0 \\ \frac{1}{4} & \frac{1}{4} & 0 & \frac{1}{2} \\ \frac{1}{4} & \frac{1}{4} & 0 & -\frac{1}{2} \end{bmatrix} \tag{13}$$

Since this matrix is not regular and its inversion is not exist, thus the amplitude ratio and phase difference are not correctly estimated. On the other hand, the coefficient matrix for 6-port B is

$$\mathbf{K}_{sa} = R_0 \cdot 10^{-4} \begin{bmatrix} \frac{1}{4} & \frac{1}{6} & \frac{1}{\sqrt{6}} & 0 \\ \frac{1}{4} & \frac{1}{6} & 0 & -\frac{1}{\sqrt{6}} \\ \frac{1}{4} & \frac{1}{6} & 0 & \frac{1}{\sqrt{6}} \\ 0 & \frac{1}{\sqrt{3}} & 0 & 0 \end{bmatrix} \tag{14}$$

which is regular and its inversion can be calculated. Thus the amplitude ratio and phase difference can be estimated.

IV. Dynamic range of 6-port

One of the shortcomings of the 6-port is its low dynamic range. In this section, the dynamic range of 6-port B is examined based on the simulations.

In Fig. 8, the output powers are shown respect to the amplitude ratio of the two input sources at $f = 1005$ MHz for 6-port B. The input signals are assumed in phase. One can see the powers at the output ports will remain unchanged if the amplitude ratio of the two input sources is large. In other words, for discriminating two signals of great difference in amplitude, the powers should be measured with great accuracy, which is usually impossible. Thus simulations are conducted to examine the the dynamic range of the 6-port. Here 6-port B in the previous section is examined.

In Figs. 6 and 7, simulations were conducted with only the power at port 2 having measurement errors. Considering the real situations, the powers at all the four ports were are assumed having random measurement errors within -0.1 to 0.1 dBm, and the errors are assumed independent with each

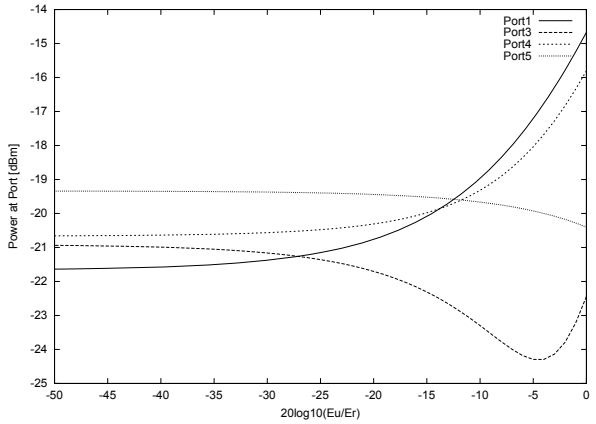

Fig. 8. The output powers versus the amplitude ratio of the two input sources at $f = 1005$ MHz for 6-port B.

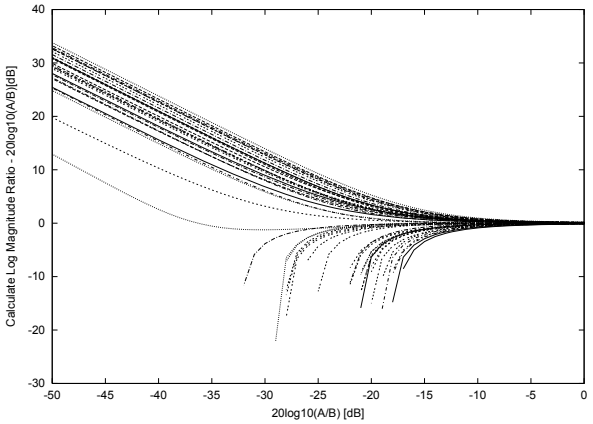

Fig. 9. The error between the estimated amplitude ratio and the real amplitude ratio versus the real amplitude ratio at $f = 1005$ MHz with random measurement errors.

other. The simulations results for 50 random cases at $f = 1005$ MHz are shown in Figs. 9 and 10. The input signals are assumed in phase. i.e., with phase difference of 0. In Fig. 9, the error between the estimated amplitude ratio and the real amplitude ratio is graphed versus the real amplitude ratio. One can see while the amplitude ratio is within -10 to 0 dB, the error between the estimated amplitude ratio and the real amplitude ratio is within ± 1 dB. While the amplitude ratio is less than -15 dB, the error will increase. From Fig. 10, one can see while the amplitude ratio is within -20 to 0 dB, the error of the estimated phase difference is less than ± 5 °. While the amplitude ratio is less than -20 dB, the error will increase. Thus for obtaining a reliable estimated results, it is better to keep the amplitude ratio of the two inputs with in -20 to 0 dB.

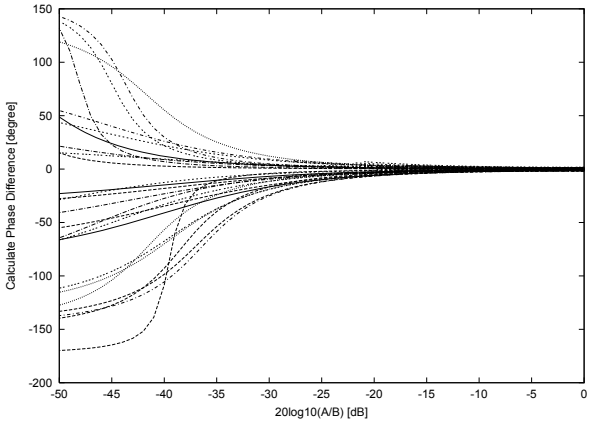

Fig. 10. The estimated phase difference versus the real amplitude ratio at $f = 1005$ MHz with random measurement errors.

V. Conclusion

Measuring the complex magnetic field by using a 6-port circuit has been discussed. Two 6-port circuits have been fabricated and examined, and problem in fabricating the 6-port circuits has been clarified. The dynamic range of the 6-port has also been investigated based on the simulations.

References

[1] T.Tobana and Y.Kami, "Measurement of Magnetic Near Field on a Printed Circuit Board of Finite Size and a Simple Estimation Method of Far Fields", The transactions of the Institute of Electronics, Information and Communication Engineers, Vol.J79-B2, No.11, pp.812- ,Nov. 1996.

[2] Y. Kami, and T. Tobana, "Measurement of magnetic near field on printed circuit boards by using a magnetic loop antenna," Proc. 12the Intn. Zurich Symp. and Tech. Exhib. Electromagn., pp.591-596, 1997.

[3] R.F.Harrington , "Time-harmonics electromagnetic fields.", McGRAW-HILL,New York,1961 sec.4

[4] H.Hirayama, Y.Kami, "Estimation of Near-E Field and Far Field Radiation Pattern with Only Near-M Field Measurement Using Yee Scheme", Technical report of IEICE, EMCJ2002-73, 2002-10.

[5] Y.Imamura, Fengchao XIAO, K.Murano, Y.Kami, "COMPENSATION OF LOOP PROBE FOR NEAR-MAGNETIC FIELD MEASUREMENT USING IMAGE RESTORATION TECHNIQUE," Society Conference of IEICE, B-4-65, 2005.9.

[6] S.Kazama, K.Arai, "Sensing model for electrmagnetic sensor measuring electric and magnetic field distributions", Technical report of IEICE, EMCJ2001-115, 2002-03.

[7] E.suzuki, T.Miyakawa, H.Ota, K.Arai, "Characteristics of an Optical Magnetic Probe Consisting of a Loop Antenna Element and a Bulk Electro-Optic Crystal", Technical report of IEICE, EMCJ 2002-19, 2002-06.

[8] H. Hirayama, H. Kondo, N. Kikuma, and K. Sakakibara," Visualization of emission from bend of a transmission line with Poynting vector and wave-number vector," Proc. of EMC Europe 2008, pp.143-146, Hamburg, Germany, Sept. 2008.

[9] A.Ogata, K.Fujii, Y.Matumoto, A.Sugiura, "Amplitude/Phase Measuring System for EM Noise in Microwave Band", Society Conference of IEICE, B4-5, 2005-9.

[10] G.F.Engen," The six-port reflectmeter : An alternativr network analyzer", IEEE Transactions on microwave theory and techniques, VOL. MTT-25,No.12,pp.1075-1080,Dcember 1977

[11] G.F.Engen,"An Improved circuit for implementing the six-port technique of microwave measurements", IEEE Transactions on microwave theory and techniques, VOL. MTT-25,No.12,pp.1080-1083,Dcember 1977